Earthquake-induced transformation of the lower crust

Bjørn Jamtveit[1], **Yehuda Ben-Zion**[2], **François Renard**[1,3], and **Håkon Austrheim**[1]

[1]Physics of Geological Processes (PGP), The Njord Centre, Department of Geosciences, University of Oslo, P.O. Box 1048, Blindern, 0136 Oslo, Norway

[2]Department of Earth Sciences, University of Southern California, Los Angeles, CA 90089, U.S.A.

[3]Univ. Grenoble Alpes, Univ. Savoie Mont Blanc, CNRS, IRD, IFSTTAR, ISTerre, 38000 Grenoble, France

Abstract

The structural and metamorphic evolution of the lower crust has first order effects on the lithospheric response to plate tectonic processes involved in orogeny, including subsidence of sedimentary basins, stability of deep mountain roots, and extension of high topography regions. Recent research shows that prior to orogeny most of the lower crust is dry, impermeable, and mechanically strong1. During an orogenic event, the evolution of the lower crust is controlled by infiltration of fluids along localized shear or fracture zones. In the Bergen Arcs of Western Norway, shear zones initiate as faults generated by lower crustal earthquakes. Seismic slip in the dry lower crust requires stresses at a level that can only be sustained over short timescales or local weakening mechanisms. However, regular earthquake activity in the seismogenic zone produces stress pulses that drive aftershocks in the lower crust2. Here, we show that the volume of lower crust affected by such aftershocks is very significant and that fluids driving associated metamorphic and structural transformations of the lower crust follow in the wake of these earthquakes. This provides a novel 'top-down' effect on crustal geodynamics and connects processes operating at very different time scales.

The structural and metamorphic evolutions of the lower crust are key elements in the dynamics of the lithosphere. Frequent observations of fluid-induced metamorphism associated with ductile deformation along shear zones on scales ranging from millimeters to kilometers inspired early models of the lithosphere such as the 'jelly-sandwich' model3. In this model, the lower crust is assumed to be wet and mechanically weak, and plate tectonic stress is transmitted through the brittle upper crust and a strong upper mantle. This model

was challenged[4] with the argument that a strong lower crust is essential for the survival of thick mountain roots and high mountains. The lower crust is dominated by granulite facies rocks of mafic to intermediate composition[5] and such rocks will be nominally dry at normal steady state geothermal gradients for a wide range of crustal heat flow and heat production conditions[1]. Hence, the rheology of the lower crust *prior to* an orogeny will in most cases be controlled by the properties of dry mineral assemblages dominated by plagioclase, pyroxene, garnet and olivine, with plagioclase being the most abundant phase. This is consistent with the estimated viscosity of the lower crust ($\sim 10^{24}$ Pa·s) required to generate the crustal support needed for intraplate seismicity such as the 2001 M_W 7.6 Bhuj earthquake in western India[6]. Recent modeling[7] furthermore suggests that the Indian lower crust remains strong beneath the entire southern half of the Tibetan plateau.

Observations on structural and metamorphic transformation of initially dry lower crust during orogenic events indicate an early stage involving seismic failures[8–10]. Metamorphism and shear zone development then follow in the wake of lower crustal earthquakes. These observations raise an enigma that has so far been unresolved, because frictional failure of dry rocks at the confining pressures of the lower crust (~ 1 GPa) requires differential stress levels exceeding 2 GPa[11]. Although dry plagioclase-dominated rocks deforming by dislocation creep can in theory develop extremely high differential stress at lower crustal temperatures and high strain rates, the stress level that can be sustained over orogenic time scales for reasonable strain rates in coherent crustal volumes will be far below what is required for brittle faulting (< 1 GPa, see Methods). Deep crustal earthquakes occurring under constant loading in intact rocks thus seem to require a local weakening mechanism.

During subduction of the Indian plate under south Tibet, earthquakes occur at 60-100 km depth (Fig.1), but are confined to regions very close to the Mohorović discontinuity (Moho) at temperatures below 600°C[7]. Interestingly, the pressure and temperature conditions in the region where these earthquakes nucleate overlap the conditions at which serpentine breaks down to produce hydrous fluids in mantle rocks. Fluid production near the Moho can both reduce effective pressures and weaken the crust and mantle by mineral transformation processes and thus be a plausible explanation for the observed seismic activity.

In the absence of such local weakening mechanisms, seismic deformation in the lower crust may be driven by transient 'stress pulses' [6,10,13]. Here we propose that regular earthquakes in the brittle upper crust provide a natural mechanism for sustained generation of stress pulses and associated seismic failures in the lower crust. During the occurrence of large earthquakes the strain rates around and below the rupture area increase by many orders of magnitudes. A representative strain accumulation of 15 mm per year across a width comparable to a geodetic locking depth of 15 km corresponds to an interseismic strain rate of $3 \cdot 10^{-14}$/s. In contrast, seismic slip velocities of 1-10 m/s across rupture localization width of 1-10 mm lead to seismic strain rates of 10^3-10^4/s. Such large co-seismic jumps can explain a transient increase in seismic rupture within the lower crust.

Observational evidence for very high, short-lived, stresses in the lower crust come from the occurrence of fossil earthquakes. A recent study of the Woodroffe Thrust located within the Musgrave Block in Central Australia[14] documents the formation of large volumes of pseudotachylytes in completely dry lower crustal granulites. Stress levels exceeding 0.5 GPa have also been inferred from lower crustal earthquakes leading to pseudotachylyte formation in gabbros and ultramafic rocks in the Alpine subduction complex of Corsica, France[15].

Simulated deformation on faults using various versions of rate- and state-dependent friction models show that large earthquake slip penetrates into the nominally stable deeper region[16,17]. Simulations of aftershocks in a viscoelastic damage model consisting of a brittle upper crust over a lower crust with power-law viscosity constrained by laboratory experiments indicate that the hypocenters of early aftershocks are significantly deeper than the regular seismogenic zone[2]. Depending on model parameters and thermal gradients, the maximum depth of the early aftershocks can approach twice that of the usual seismicity. Details of these results depend on the employed constitutive laws and parameters, but lower crustal aftershocks are generic outcomes of the high strain rates generated by large earthquakes at the bottom of the seismogenic zone.

Below we use basic scaling relations to demonstrate that observed worldwide earthquake activity in the regular seismogenic zone of subduction zones and seismically active continental regions is expected to produce considerable fracture area and rupture zone volume in the lower crust. This, in turn, generates transient pathways for fluids from the wet upper crust above, or the slab below, to the dry lower crust (Fig. 1). Fluids play a key role in the long-term evolution of the lower crust[1]. As an example, we describe earthquake-triggered eclogite-facies metamorphism and shear zone development of lower crustal granulites from the Bergen Arcs in Western Norway (Fig. 2A). The observations highlight the close association between earthquakes, fluid migration and transformation processes in the lower crust.

The Bergen Arcs represent a series of thrust sheets where granulite facies remnants of Proterozoic lower crust recrystallized to an anhydrous mineralogy at 930 Ma[18]. During the Caledonian continent-collision between Laurentia and Baltica between 420 and 440 Ma[18], fluid-induced metamorphic transformations formed eclogites and amphibolites in shear zones, breccias and along fractures. The estimated eclogitization conditions are ca. 670-690°C and 2.1-2.2 GPa[19]. Pseudotachylytes, fine-grained or glassy fault rocks believed to reflect earthquake related frictional melting, are abundant on faults where granulites facies rocks experienced Caledonian retrograde metamorphism (Fig. 2A). Such faults show single rupture displacements reaching 1.7 m (Fig. 2B), corresponding to an earthquake exceeding magnitude 7. Single pseudotachylyte veins range in thickness from millimeters to a few centimeters (Fig. 2C), and also occur as a thin 'matrix' between rotated blocks of brecciated granulite that sometimes cover areas exceeding 100 m^2. Microstructures developing in the fault wall rocks display intense fragmentation without significant shear strain[22], followed by healing processes through grain growth and formation of eclogite facies minerals, including hydrous phases such as amphibole, mica and clinozoisite. Infiltration of hydrous fluids was thus directly associated with seismic slip.

A significant rheological weakening associated with formation of the fine-grained and hydrous eclogite often leads to development of ductile shear zones in areas initially deformed by brittle failure. Relict pseudotachylytes can occasionally be observed 'floating' in the shear zones, providing unambiguous evidence for ductile deformation predated by brittle failure of granulite facies rocks (Fig. 3). In the following, we explore the feasibility that lower crustal earthquakes, such as those described, are aftershocks triggered by stress pulses generated by mainshocks in the normal seismogenic regime of a plate boundary.

Basic seismological scaling relations provide an order-of-magnitude estimate of the lower crustal rock volume affected by aftershocks. We demonstrate that this is significant, with conservative parameter values and ignoring probable contributions from penetration of large mainshocks into the lower crust as well as ductile/thermal instabilities[16,17].

Lower crustal earthquakes are not expected to occur repeatedly in the same location because rock melting and subsequent solidification is a strengthening process[23]. This is consistent with observations of distributed "fields" of pseudotachylytes (Fig. 2A), each associated with a single event. The total volume of rock damage V_{RD} produced by crustal earthquakes in the magnitude range $M_1 < M < M_2$ is then given by

$$V_{RD} = \int_{M_1}^{M_2} A(M) \cdot t_{RD}(M) \cdot n(M) dM . \quad (1)$$

Here $A(M)$ is the rupture area of an earthquake with magnitude M, $t_{RD}(M)$ is the damage zone thickness around the rupture area and $n(M)$ is the event density given by the Gutenberg-Richter relationship

$$\log_{10} n(M) = a - bM, \quad (2)$$

where a and b are empirical constants. The scaling relations for $A(M)$ and $t_{RD}(M)$ are found using basic theoretical relations from fracture mechanics[24,25] and empirical relation between the magnitude and potency of earthquakes[26,27] (see Methods). An explicit relationship for the total volume of damage produced by earthquakes in the considered magnitude range can be expressed as:

$$V_{RD}(M_1 < M < M_2) = \beta \cdot [e^{\alpha M_2} - e^{\alpha M_1}], \quad (3)$$

where α and β are positive parameters that account for the combined scaling relations of A, t_{RD} and n with M[24–27]. By using observationally-constrained parameters, the volume of rock damaged by crustal earthquakes is estimated to be $V_{RD} = 1.2 \cdot 10^{-5}$ km^3 per year per km^2 of the Earth's surface in the seismically active region (see Methods). For the lower magnitude limit we use $M_1 = 0$ with slip distance of the order of the grain size of granulites. For an upper limit relevant to the lower crust we take $M_2 = 8.3$ since the largest subduction zones events can have M 9.5, and the largest aftershock magnitude is typically ~1.2 units

below that of the mainshock[28,29]. The parameters of the Gutenberg-Richter relationship are taken from recent analysis of global earthquakes with depths less than 70 km[30]. Analysis of earthquake clusters indicates[29,30] that ~75% of all events with $M > 0$ are aftershocks. We therefore use 75% of the observed intensity of events[30] to estimate the average annual production of damaged rock volume by aftershocks with $0 < M < 8.3$. Based on previously conducted simulations[2] we assume conservatively that 1% of the aftershock population is in the lower crust. The estimated annual production of rupture zone volume in the lower crust is then $1.2 \cdot 10^{-7}$ km^3/yr per km^2 area at the Earth surface.

For a concrete example, Western Norway was an active subduction zone during the Caledonian orogeny for $>2 \cdot 10^6$ yr. Based on the estimates above, the total seismically damaged volume in the lower crust of Western Norway is estimated to be 0.24 km^3 per km^2 area at the Earth surface. For a 20 km thick lower crust, this implies a rupture zone volume exceeding 1.2% of the total lower crustal volume. The Bergen Arcs example demonstrates that in the presence of fluids, lower crustal earthquakes initiate metamorphism of rock volumes typically 1-2 orders of magnitude larger than that of the rupture zone (i.e. a 0.1-1 m thick eclogite forming around 1 cm thick rupture zone). Hence the overall process can alter a large fraction of the lower crust. The sensitivity of the results to input parameters is discussed in the Methods section and shows that the 1.2% estimate of lower crust volume damaged by earthquakes is based on conservative values of input parameters and is likely to be higher.

Our results indicate that aftershocks triggered by major earthquakes in the regular seismogenic zone have the potential to initiate pervasive transformation of the lower crust on a timescale of 10^6 years. Direct recording of a transient deepening of early aftershocks requires a dense observational network around large mainshock ruptures. Although this situation is not often met, such lower crust aftershocks are sometimes observed. Recent examples of deep aftershocks include the 2001 M_W 7.6 Bhuj intraplate earthquake in India where aftershocks occurred down to Moho depths[6], and the 2015 M_W 7.8 Gorkha earthquake in Nepal where the hypocenter occurred near the Main Himalayan Thrust at a depth of 10-15 km[12] and aftershocks penetrated the Indian crust to a depth exceeding 30 km (Fig. 1A).

Earthquakes in dry lower crust driven by stress pulses generated in the seismogenic zone have a number of important consequences, many of which are illustrated by the Bergen Arcs example. The most important is arguably the associated increase in permeability which may connect the dry lower crust to an external fluid reservoir. In the Bergen Arcs, pseudotachylyte formation is always associated with influx of hydrous fluids[21]. Fluid driven metamorphic reactions are fast due to the metastable state of the granulite facies rocks[1], leading to a profound reduction in rock strength and the development of shear zones and ductile deformation at lower stress levels[31,32]. The positive feedbacks between fluid introduction, weakening, and shear zone development eventually produce a complete transformation of large volumes of lower crust from a low density, dry and strong lithology, to a high density, wet and weak one. Thus even in situations where aftershocks directly affect only limited volumes of lower crust, they may start a series of fluid-induced transformation processes which can effect far bigger volumes.

The 'top-down' control on lower crustal evolution presented here challenges the traditional 'bottom-up' view where deep shear zones are assumed to control the spatial distribution of faults above the brittle-ductile transition. Generation of deep crustal shear zones as a response to weakening induced by pre-existing faults triggered by stress pulses generated by shallower earthquakes may also explain observed fluids with meteoric and other upper crustal signatures, such as the presence of hydrocarbons, in shear zones formed below the brittle-ductile transition33.

Methods

Controls on lower crustal stress levels

Flow law creep parameters for synthetic plagioclase aggregates for variable water contents were presented by Rybacki and Dresen34. Extended Data Fig.1 shows the relations between temperature, strain rate and differential stress for water poor plagioclase aggregates based on these experimental data. At 660-680°C, the estimated temperature during seismic faulting in the Bergen Arcs, the maximum differential stress developing for a strain rate of 10^{-14} s^{-1} would be ca. 0.3 GPa and clearly insufficient to cause brittle failure. Such strain rates would probably only apply within zones where strain was already localized. In a coherent crustal volume, the internal strain rate would be far less. Craig et al7., estimate strain rates at around 10^{-16} s^{-1} for the subducting Indian plate beneath eastern Tibet. Even if local strain rate increases should be able to push stress levels beyond what would be expected in coherent crustal slabs, or if the crustal temperature was lower than for the Bergen case so that the effective viscosity was higher, stresses much higher than 1 GPa would be unrealistic due to the onset of Peierls creep35, or even cataclastic flow36.

Volume of damage produced by earthquakes

The step-by-step derivation of Equation (3) and the calculation of the volume of rock damaged by earthquakes in the crust, V_{RD}, are detailed here. The total volume of rock damage produced by crustal earthquakes in the magnitude range $M_1 < M < M_2$ is given by

$$V_{RD} = \int_{M_1}^{M_2} A(M) \cdot t_{RD}(M) \cdot n(M)dM . \quad (S1)$$

Each term in the integral is described below.

The density of events $n(M)$ in (S1) is provided by the Gutenberg-Richter relationship

$$\log_{10}n(M) = a - bM, \quad (S2)$$

where a and b are empirical constants.

Assuming that each earthquake is approximately a circular rupture with radius r and surface area $A = \pi r^2$ that sustains a uniform strain drop e, the seismic potency, P_0, (moment/rigidity) is given by24,

$$P_0 = (16/7) \cdot \Delta \varepsilon \cdot r^3 . \quad \text{(S3)}$$

The seismic potency and magnitude of earthquakes spanning a relatively small range (4) of magnitudes are related empirically by a relation of the type[26,27],

$$\log_{10} P_0 = d \cdot M + e, \quad \text{(S4)}$$

with potency units in $km^2 \cdot cm$ and constants d and e.

Combining Eqs. (S3) and (S4), the radius of an earthquake with magnitude M in unit of km is:

$$r(M) = \left[\frac{7 \cdot 10^{-5}}{16 \Delta \varepsilon} \right]^{1/3} \cdot 10^{((d \cdot M + e)/3)}, \quad \text{(S5)}$$

where the 10^{-5} factor account for unit conversion of P_0 from $km^2 \cdot cm$ to km^3. Using (S5) for r and assuming again a circular crack such that $A(M) = \pi r^2$, one obtains

$$A(M) = \pi \left[\frac{7 \cdot 10^{-5}}{16 \Delta \varepsilon} \right]^{2/3} \cdot 10^{(2(d \cdot M + e)/3)} . \quad \text{(S6)}$$

The thickness of the damage zone, t_{RD}, is expected from fracture mechanics to scale linearly with the rupture radius[25].

$$t_{RD}(M) = \gamma \cdot r(M), \quad \text{(S7)}$$

where the constant γ is proportional to the dynamic stress intensity factor and the ratio of stress drop over strength drop. For standard rupture velocity of 0.9 times the Rayleigh wave speed and a stress drop that is 10% of the strength drop, $\gamma \sim 10^{-2} - 10^{-3}$ (situations with relatively high initial stress leading to higher stress drop give higher γ values). Here we conservatively use $\gamma = 0.002$.

Combining (S2), (S6) and (S7) leads to

$$A(M) \cdot t_{RD}(M) \cdot n(M) = \pi \cdot \gamma \cdot \left[\frac{7 \cdot 10^{-5}}{16 \Delta \varepsilon} \right] \cdot 10^{((d-b) \cdot M + e + a)} . \quad \text{(S8)}$$

Integrating (S1) using (S8) gives an explicit relationship for the total volume of damage produced by earthquakes in the form

$$V_{RD}(M_1 < M < M_2) = \beta[e^{\alpha M_2} - e^{\alpha M_1}] \quad \text{(S9)}$$

where $a = (d - b)ln(10)$ and $\beta = \frac{\pi}{\alpha}\gamma 10^{a + e}\left(\frac{7 \cdot 10^{-5}}{16 \Delta \varepsilon}\right)$ are positive parameters and V_{RD} is in

unit of km^3 per year per km^2 of the Earth's surface in a seismically active region.

Observed b-values are typically around 1 while a-values vary significantly with space and time. We focus on deformation in subduction zones and seismically active continental regions and use average a and b values based on analysis of global earthquakes with depth shallower than 70 km during 1975-2015 in the Northern California Earthquake Data Center (NCEDC) catalog30. From Fig. 1 of Ref. [30] and a b-value of 1, a representative intensity of events with $M > 0$ (10^a) in active subduction zones is 6/(yr·km^2), corresponding to $a = log_{10}(6) = 0.78$. This value is conservative since the NCEDC catalog does not include numerus small events buried in the coda of larger events and noise. The results of Ref. [30] indicate that about 50% of $M > 4$ events in subduction zones and continental transform regions are aftershocks. The fraction of events that are aftershocks increases as the event magnitude decreases29,30, so we assume that ~75% of all events with $M > 0$ are aftershocks. The event intensity 10^a used below to estimate damaged rock volume by aftershocks is reduced accordingly by a factor of 0.75 from 6 to 4.5.

Analysis of earthquakes in southern California recorded by the regional network and borehole sensors indicates26 that $d = 1$ and $e = -4.7$ for $M < 3.5$ while $d = 1.34$ and $e = -5.22$ for $M > 3.5$. Similar constants characterize earthquakes in other locations27. Inserting into Eq. (S8) these constants d and e for $0 < M < 3.5$ and $3.5 < M < 8.3$ magnitude ranges, a more explicit expression of volume of damaged rocks (in km^3 per yr per km^2 of the Earth's surface at the seismically active region) is

$$V_{RD} = \int_{M_1}^{M_2} A(M) \cdot t_{RD}(M) \cdot n(M)dM = \pi \cdot \gamma \cdot \left[\frac{7 \cdot 10^{-5}}{16 \Delta \varepsilon}\right] \cdot 10^a \cdot \int_{M1}^{M_2} 10^{((d-b) \cdot M + e)}dM \text{ (S10)}$$

and

$$V_{RD} = \pi \cdot \gamma \cdot \left[\frac{7 \cdot 10^{-5}}{16 \Delta \varepsilon}\right] \cdot 10^a \cdot \left\{\int_0^{3.5} 10^{-4.7}dM + \int_{3.5}^{8.3} 10^{0.34M} \cdot 10^{-5.22}dM\right\} \quad \text{(S11)}$$

Evaluating (S10) and (S11) gives $V_{RD} = 1.2 \ 10^{-5}$ km^3 per year per km^2 of the Earth's surface in a seismically active region.

The fraction of lower crust volume affected by earthquake ruptures (1.2%) is obtained using $10^a = 4.5$, $\varepsilon = 5 \cdot 10^{-5}$ and the values of other constants mentioned in the text. The result is sensitive to the input parameters, but it is based on realistic values of earthquake intensities in active subduction zones (4.5 annual aftershocks with $M > 0$ per km^2), assumed lower and

upper limits of aftershock magnitudes (0 and 8.3), average strain drop ($\varepsilon = 5 \cdot 10^{-5}$), ratio of damage zone thickness to rupture radius $\gamma = 0.002$, and the fraction of aftershocks with hypocenters in the lower crust (1%). Reducing the lower magnitude limit will increase significantly the rupture surface area but not change much the estimated damage zone volume; decreasing the upper magnitude limit from 8.3 to 7.8 will decrease the estimated volume of damaged rock by 32%. Changing the assumed average strain drop $\varepsilon = 5 \; 10^{-5}$ to average strain drops of $5 \; 10^{-4}$ and $5 \; 10^{-6}$ will modify the estimated damage volume by factors of 0.21 and 4.64, respectively. Changing γ or the deformation time scale by a given factor (e.g. 2) will modify the damage volume by the same factor. As a consequence, reasonable variations of these parameters will not change significantly the estimated lower crust volume affected by earthquake ruptures.

Extended Data
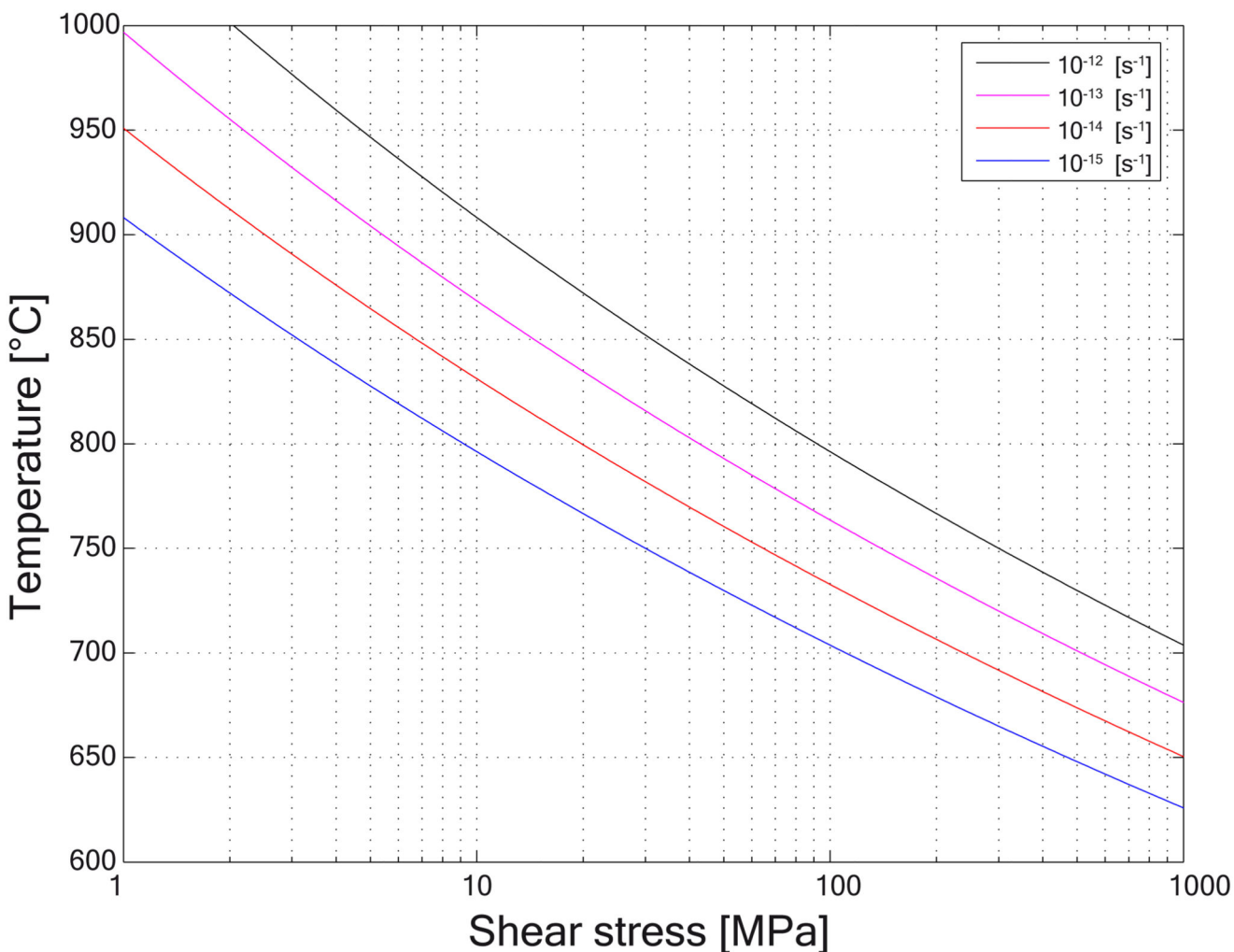
Extended Data Figure 1. Rheology of dry anorthite.
Shear stress versus temperature diagram contoured with respect to strain rate.

Acknowledgements

References

1. Jamtveit B, Austrheim H, Putnis A. Disequilibrium metamorphism of stressed lithosphere. Earth-Science Reviews. 2016; 154:1–13.

2. Ben-Zion Y, Lyakhovsky V. Analysis of aftershocks in a lithospheric model with seismogenic zone governed by damage rheology. Geophysical Journal International. 2006; 165:197–210.

3. Chen WP, Molnar P. Focal depths of intracontinental and intraplate earthquakes and their implication for the thermal and mechanical properties of the lithosphere. Journal of Geophysical Research. 1983; 88:4183–4214.

4. Jackson J. Strength of the continental lithosphere: Time to abandon the jelly sandwich? GSA Today. 2002; 12

5. Rudnick RL, Fountain DM. Nature and composition of the continental lower crust. Reviews in Geophysics. 1995; 33:267–309.

6. Copley A, Avouac J-P, Hollingsworth J, Leprince S. The 2001 M_W 7.6 Bhuj earthquake, low fault friction and the upper crustal support of plate driving forces in India. Journal of Geophysical Research. 2011; 116 B08405.

7. Craig TJ, Copley A, Jackson J. Thermal and tectonic consequences of India underthrusting Tibet. Earth and Planetary Science Letters. 2012; 353–354:231–239.

8. Austrheim H, Boundy TM. Pseudotachylytes generated during seismic faulting and eclogitization of the deep crust. Science. 1994; 265:82–83. [PubMed: 17774692]

9. John T, Schenk V. Interrelations between intermediate-depth earthquakes and fluid flow within subducting oceanic plates: Constraints from eclogite facies pseudotachylytes. Geology. 2006; 34:557–560.

10. Moecher DP, Steltenpohl MG. Direct calculation of rupture depth for an exhumed paleoseismogenic fault from mylonitic pseudotachylyte. Geology. 2009; 37:999–102.

11. Kohlstedt DL, Evans B, Mackwell S. Strength of the lithosphere – constraints imposed by laboratory experiments. Journal of Geophysical Research. 1995; 100:17587–17602.

12. McNamara DE, Yeck WL, Barnhart WD, Schulte-Pelkum V, Bergman E, Adhikari LB, Dixit A, Hough SE, Benz HM, Earle PS. Source modeling of the 2015 M_W 7.8 Nepal (Gorkha) earthquake sequence: Implications for geodynamics and earthquake hazards. Tectonophysics. 2017; 714–15:31–30.

13. Ellis S, Stöckhert B. Elevated stresses and creep rates beneath the brittle-ductile transition caused by seismic faulting in the upper crust. Journal of Geophysical Research. 2004; 109 B05407.

14. Hawemann F, Mancktelow NS, Wex S, Camacho A, Pennaccioni G. Pseudotachylyte as field evidence for lower crustal earthquakes during the intracontinental Petermann Orogeny (Musgrave Block, Central Australia). Solid Earth Discuss. 2017; doi: 10.5194/se-2017-123

15. Andersen TB, Mair K, Austrheim H, Podladchikov YY, Vrijmoed JC. Stress release in exhumed intermediate and deep earthquakes determined from ultramafic pseudotachylite. Geology. 2008; 36:995–998.

16. Hillers G, Ben-Zion Y, Mai PM. Seismicity on a fault controlled by rate- and state dependent friction with spatial variations of the critical slip distance. Journal of Geophysical Research. 2006; 111 B01403.

17. Jiang J, Lapusta N. Connecting depth limits of interseismic locking, microseismicity, and large earthquakes in models of long-term fault slip. Journal of Geophysical Research. 2017; 122doi: 10.1002/2017JB014030

18. Bingen B, Davis WJ, Austrheim H. Zircon U-Pb geochronology in the Bergen arc eclogites and their Proterozoic protoliths, and implications for the pre-Scandian evolution of the Caledonides in western Norway. Geological Society of America Bulletin. 2001; 113:640–649.

19. Bowany K, Hand M, Clark C, Kelsey DE, Reddy SM, Pearce MA, Tucker NM, Morrissey J. Phase equilibira modelling constraints on P-T conditions during fluid catalysed conversion of granulite to eclogite in the Bergen Arcs, Norway. Journal of Metamorphic Geology. 2017; doi: 10.1111/jmg. 12294

20. Austrheim H. Fluid and deformation induced metamorphic processes around Moho beneath continent collision zones: Examples from the exposed root zone oft he Caledonian mountain belt, W-Norway. Tectonophysics. 2013; 609:620–635.

21. Wells DL, Coppersmith KJ. New empirical relationships among magnitude, rupture length, rupture width, rupture area, and surface displacement. Bulletin of the Seismological Society of America. 1994; 84:974–1002.

22. Austrheim H, Dunkel KG, Plümper O, Ildefonse B, Liu Y, Jamtveit B. Microstructural records of seismic slip. Science Advances. 2017; 3:e1602067. [PubMed: 28261660]

23. Mitchell TM, Toy V, Di Toro G, Renner J, Sibson RH. Fault welding by pseudotachylyte formation. Geology. 2016; 44:1059–1062.

24. Ben-Zion Y. Collective behavior of earthquakes and faults: Continuum-discrete transitions, progressive evolutionary changes and different dynamic regimes. Reviews in Geophysics. 2008; 46:RG4006.

25. Ben-Zion Y, Ampuero J-P. Seismic radiation from regions sustaining material damage. Geophysical Journal International. 2009; 178:1351–1356.

26. Ben-Zion Y, Zhu L. Potency-magnitude scaling relations for southern California earthquakes with $1.0 < M_L < 7.0$. Geophysical Journal International. 2002; 148:F1–F5.

27. Edwards B, Allmann B, Fah D, Clinton J. Automatic computation of moment magnitudes for small earthquakes and the scaling of local to moment magnitude. Geophysical Journal International. 2010; 183:407–420.

28. Båth M. Lateral inhomogeneities in the upper mantle. Tectonophysics. 1965; 2:483–514.

29. Zaliapin I, Ben-Zion Y. Earthquake clusters in southern California Identification and stability. Journal of Geophysical Research. 2013; 118:2847–2864.

30. Zaliapin I, Ben-Zion Y. A global classification and characterization of earthquake clusters. Geophysical Journal International. 2016; 207:608–634.

31. Putnis A, Jamtveit B, Austrheim H. Metamorphic processes and seismicity: The Bergen Arcs as a natural laboratory. Journal of Petrology. 2017; 58:1871–1898.

32. Yardley BWD. The role of water in the evolution of the continental crust. Journal of the Geological Society. 2009; 166:585–600.

33. Munz IA, Yardley BWD, Banks D, Wayne D. Deep penetration of sedimentary fluids in basement rocks from Southern Norway – Evidence from hydrocarbon and brine inclusions in quartz veins. Geochimica et Cosmochimica Acta. 1995; 59:239–254.

34. Rybacki E, Dresen G. Deformation mechanism maps for feldspar rocks. Tectonophysics. 2004; 382:173–187.

35. Azuma S, Katayama I, Nakakuki T. Rheological decoupling at the Moho and implications to Venusian tectonics. Scientific Reports. 2014; 4:4403. [PubMed: 24638113]

36. Tullis, J., Yund, R. The brittle-ductile transition in feldspar aggregates. An experimental study. Fault mechanics and transport properties of rocks. Evans, B., Wong, T-f, editors. Academic press; 1992.
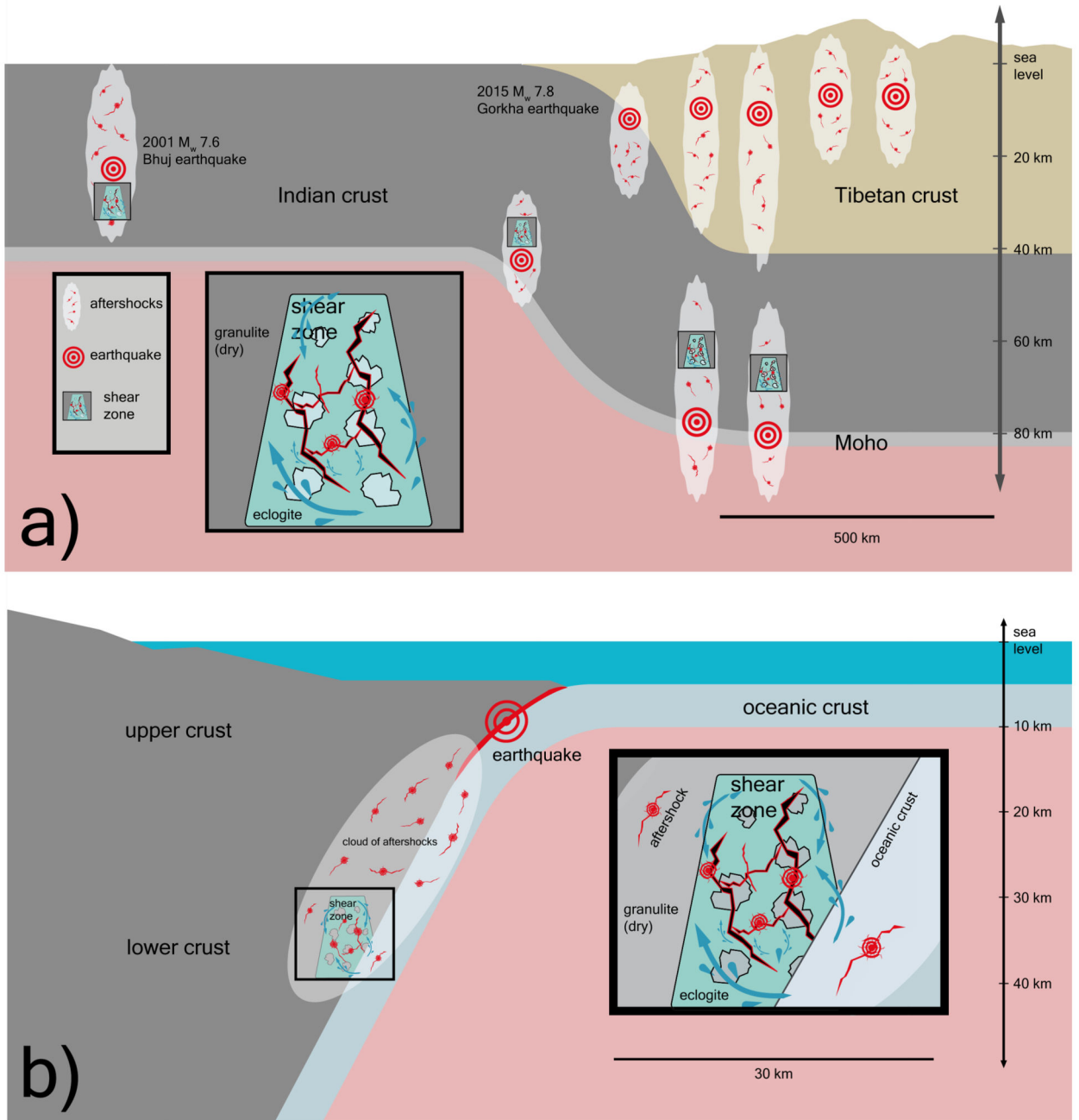
Figure 1. Earthquakes and aftershocks in the lower crust.
a, Schematic representation of earthquakes and aftershocks for the India-Tibet continent-continent collision. **b,** A generic subduction plate boundary geometry. Each major earthquake generates a cloud of aftershocks, some of which are in the lower crust (many aftershocks in the upper crust are not shown in these simple diagrams). These aftershocks create pathways for fluids (blue arrows in insets), allowing partial hydration and metamorphism of the strong and dry granulites into wet and weaker eclogites and amphibolites. This process also facilitates the development of shear zones in the continental

lower crust. For the subduction geometry, fluids could originate from the slab below or from the upper crust above. For the continental collision below the Himalayas, fluids introduced to the subducted Indian plate could originate from the dehydration of serpentine rocks below. The 2001 Bhuj[6] and 2015 Gorkha[12] earthquakes both have aftershock 'clouds' propagating down to the lower crust, potentially allowing downward migration of fluids from the upper crust.
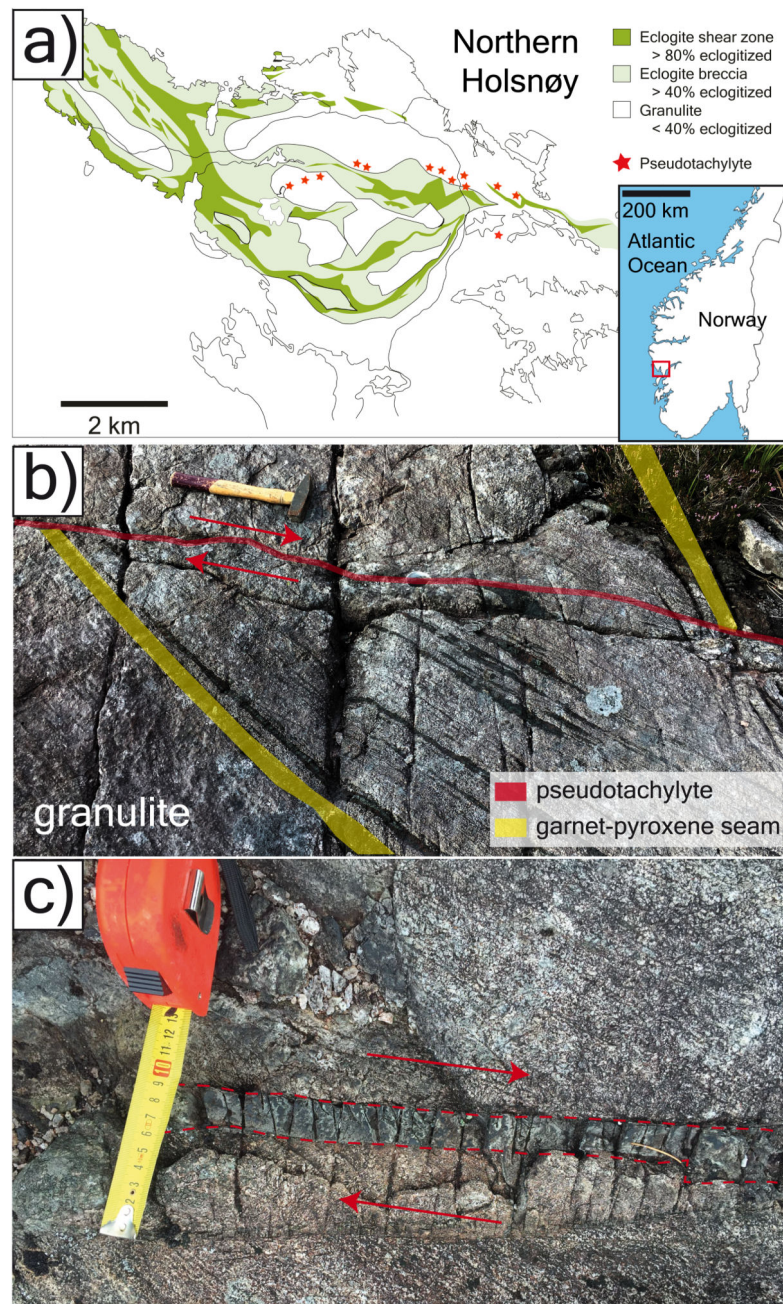
Figure 2. Fossil earthquakes in the Bergen Arcs.
a, Map of the Northwestern part of Holsnøy island in the Bergen Arcs, Western Norway (modified from Ref. 20) showing the location of pseudotachylytes (red stars) recording numerous fossil earthquakes near the transition between 940 Ma old dry lower crustal granulites and hydrated 430 Ma old eclogites. **b,** Offset of a pyroxene-rich seam by a single lower crustal earthquake. The slip surface is decorated with a melt layer, (pseudotachylyte) indicative of seismic slip. An offset of 1.7 m corresponds to a fossil earthquake with $M \approx 7$ based on the scaling relations provided in Ref. 21. **c,** Higher resolution image of the

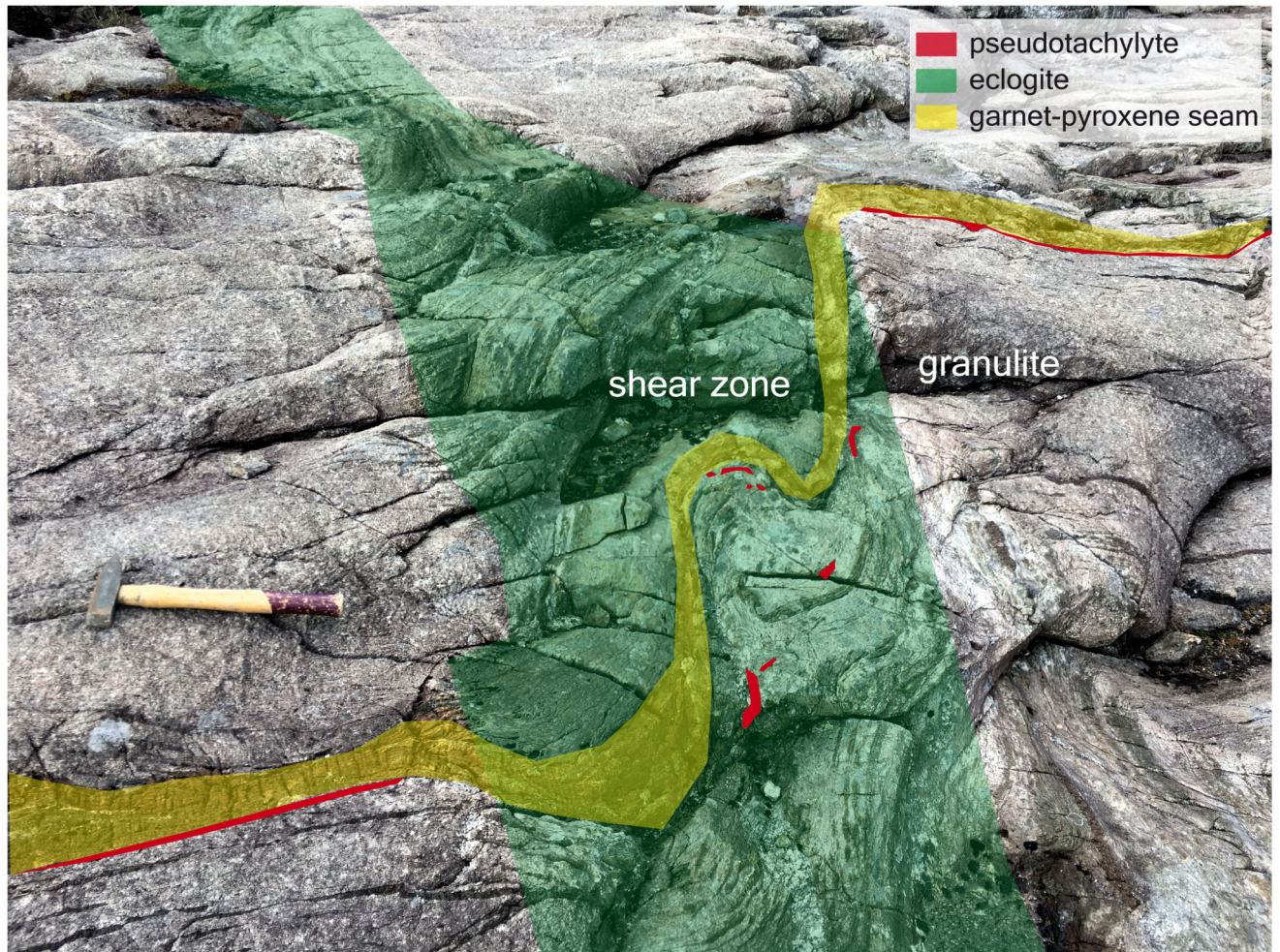centimeter-thick melt layer between the two red dashed lines. Red arrows indicate the sense of slip.

Figure 3. Transformation of the lower crust.
Offset of a pseudotachylyte by a shear zone where dry granulite rocks are transformed into wet eclogites. The earthquake occurred before the eclogitization and likely created the pathways for fluids that triggered rock transformation. Note the remains of the pseudotachylyte inside the eclogite shear zone.